Asian Journal of Chemistry; Vol. 35, No. 7 (2023), 1665-1671

ASIAN JOURNAL OF CHEMISTRY

https://doi.org/10.14233/ajchem.2023.27951

A Rhodamine Based Fluorometric and Colorimetric Probe for Detection of pH in Aqueous Medium

SUBHODIP SAMANTA

Department of Chemistry, Maulana Azad College, Kolkata-700013, India

Corresponding author: E-mail: subhodip.samanta@gmail.com

Received: 30 April 2023; *Accepted*: 27 May 2023; *Published online*: 6 July 2023; AJC-21289

Present study involves a rhodamine based fluorescent probe, which is reported to exhibit high fluorescence and colorimetric response in the pH range 2.0-5.5, where 55-fold fluorescence intensity change was identified with the lowering of pH of the medium. The working principle of the probe is based on its reversible structural inter-conversion between spirocyclic ring-close (non-fluorescent) and spirocyclic ringopen (fluorescent) forms of rhodamine base along with a reversible color change between colourless and pink with change in the pH medium. The closed spirocyclic form (AX) of the probe converts gradually into the spirocyclic open-ring (HAX) with increasing acidity of the medium and which in turn results in the strong orange fluorescence emission along with visible colorimetric responses. The calculated pK_a ~ 4.0 for such conversion indicates that the probe can be useful to detect the pH of the aqueous medium in the range 3.0-5.0. The probe displays high sensitivity, good photostability, and reversible pH dependence. Detailed analysis of the pH sensing capability of the probe were performed by means of UV-vis spectroscopy, steady state and time resolved fluorescence techniques and DFT/TD-DFT based theoretical calculations.

Keywords: Rhodamine, Fluorescence, Colorimetry, pH, Extreme acidity.

INTRODUCTION

Most of the *in vivo* processes, like metabolism, enzyme catalysis, apoptosis, transport of organelles, cell signaling, ion channel formation, various signaling pathways, *etc.* requires intracellular pH to be maintained in a particular range [1,2]. Although most prokaryotes suffer in extreme acidity (pH < 4) condition of the intercellular fluid, some microorganisms like *Acidophiles*, *Helicobacter pylori* and enteric pathogens survives in this extreme condition and may cause for the life-threatening diseases [1,2]. Therefore, measurement of physiological pH is very important in the field of clinical pathology [3,4]. Usual methodologies employed for pH measurement, comprising of microelectrodes and optical fiber electrodes in potentiometric and conductometric titration, have been reported to be rather incompatible for the measurement of physiological pH [4,5].

However, the optical spectroscopic methods, *viz.* fluorescence and absorption spectroscopy, are the two most suitable techniques for monitoring intercellular pH. Minute changes in the pH medium can be detected by suitably selecting a pH dependent fluorescent probe of high quantum yield and the colorimetric method can also be utilized if the probe shows pH dependent changes in its colour. This way, higher sensitivity, and optimum selectivity for the detection of *in vivo* pH can be achieved [5-11].

Several pH-responding fluorescent probes have been reported to monitor the changes in pH related to the changes in physiological and pathological conditions [5-7,12]. But fluorogenic or colorimetric pH-indicator probes have its limitations, *e.g.* low sensitivity, ultraviolet excitation profile and applicability in the pH range of 4-9 only [13-15].

In this respect, the fluorescent probes based on rhodamine core structure have exceptional photo-physical properties, such as long absorption and emission wavelengths which is extended to the visible region, high fluorescence quantum yield and large absorption coefficient and thus, rhodamine probes are very useful as fluorescent and colorimetric labelling reagents. The rhodamine based probes have spirolactam ring in its core structure and are non-fluorescent and colourless. But in acidic solution or in presence of suitable metal ions, spirolactam ring opening takes place and in the ring-open structure the rhodamine probes become highly fluorescent and display a visible colour [16,17].

Rhodamine pH-responsive probes are also suitable in the detection of low acidity of the aqueous medium. All other fluorescent probes reported to work as a pH sensor, like, green fluorescent protein and benzoxanthene cyanine-based pH-sensors work only in the higher pH range (4.0-9.0) of aqueous medium. Fluorescein or coumarin based probes are either chemically unstable under extreme acidic condition or because of presence of carboxyl or hydroxyl functional groups in their core structure their proton sensing ability is influenced by the interfering metal ions. The competition between the proton and the metal ions for the receptor site of the fluorescence probe leads to a non-linear response of the fluorescence intensity of the pH-sensor with the change in the pH of the medium [18-27]. A rhodamine-based reversible pH sensor having a high quantum yield has been reported by Tian *et al.* [18], which can monitor aqueous pH in the range of 1.0-4.0. Tan *et al.* [19] reported a pH-responsive rhodamine fluorescent probe which can work in the aqueous pH range of 1.75-2.62, and the sensing of pH is not affected by the presence of other metal ions in the medium. Another rhodamine-rhodamine-based pH probe was reported by Zhao *et al.* [24-26] where the fluorescent intensity was found to vary linearly with minor pH fluctuations within the range of 4.2-5.2.

In present work, a completely water soluble small organic fluorescent molecule 2-amino-3,6-*bis*(ethylamino)-7-dimethyl-spiroiso-indoline-1,9-xanthen-3-one (AX) is used to probe the pH of aqueous medium by employing steady state fluorescence and absorption spectroscopy. The mechanism depends on the pH induced structural interconversion between spirocyclic closed and open ring forms of rhodamine probe. The probe (AX) existing as a colourless spirocyclic closed form with non-fluorescent nature at neutral/basic pH converse gradually from to open ring form in acidic pH showing strong fluorescence with change of solution colour from colourless to pink (**Scheme-I**).

EXPERIMENTAL

All chemicals and solvents were purchased from Sigma-Aldrich Chemicals Pvt. Ltd. (India) and used without further purification. Probe 2-amino-3,6-*bis*(ethyl amino)-7-dimethyl-spiro, isoindoline-1,9-xanthen-3-one (AX) was prepared by following the procedures of Zhang *et al.* [28] and Kang *et al.* [29] and purified through recrystallization by using spectroscopic grade ethanol and dried repeatedly before use. Mili-Q Milipore® 18.2 MΩ cm water was used for the preparation of buffer solution of different pHs in all spectroscopic measurements. A 40 mM Britton-Robinson buffer comprising of H_3PO_4, H_3BO_3 and CH_3COOH mixture with variable pH from 1.5 to 7.0 were prepared by addition of suitable amount of 0.1 M HCl and/or 0.1 M NaOH solution. The pH of different buffer solutions was determined by Systronics digital pH meter (model No. 335). In all experiments, freshly prepared solutions were used at ambient temperature (25 ºC) and all the spectroscopic measurements were repeated at least three times to check the reproducibility.

UV-Vis absorption, steady state and time-dependent fluorescence studies: The UV-Vis absorption and steady state fluorescence spectra were measured by Perkin-Elmer Lambda 25 and Perkin-Elmer LS-55, respectively using quartz cell of 1 cm path length. In case of fluorescence studies, the excitation wavelength was kept at 530 nm. Time-resolved fluorescence measurements were carried out by using time correlated-single photon counting (TCSPC) techniques. Excitation was provided by a nanosecond diode (nano-LED, IBH, U.K.), which served as the light source operating at 500 nm and a TBX4 detection module (IBH, U.K.) coupled with a special Hamamatsu photo-multiplier tube (PMT) was used for the detection of fluorescence decays. The time resolution achievable with the present setup following deconvolution analysis of the fluorescence decays was ~ 100 ps. Fluorescence decays were recorded with a vertically polarized excitation beam and fluorescence was collected at the magic angel 54.7º.

Determination of fluorescence quantum yield: The fluorescence quantum yield of closed spirocyclic form (AX) was determined using the following equation [30] and rhodamine 6G in water was used as reference :

$$\left[\Phi = \frac{A_r E_s n_s^2}{A_s F_r n_r^2}\Phi r\right]$$

where A_i is the absorbance at the excitation wavelength, F_i is the integrated emission area and 'n' is the refraction index of the solvents used. Subscripts refer to the reference (r) or sample (s) compound. The AX fluorescence spectra were recorded by 530 nm excitation at 25 ºC in 40 mM Robinson buffer of pH 2.0. For 555 nm fluorescence intensity band, the determined quantum yield (ϕ_F) was about 0.5.

Theoretical calculation: Ground state geometries of AX and its corresponding protonated species (HAX) in the gas phase were fully optimized by density function theories (DFT) using Gaussian 09 program [31]. The B3LYP function with

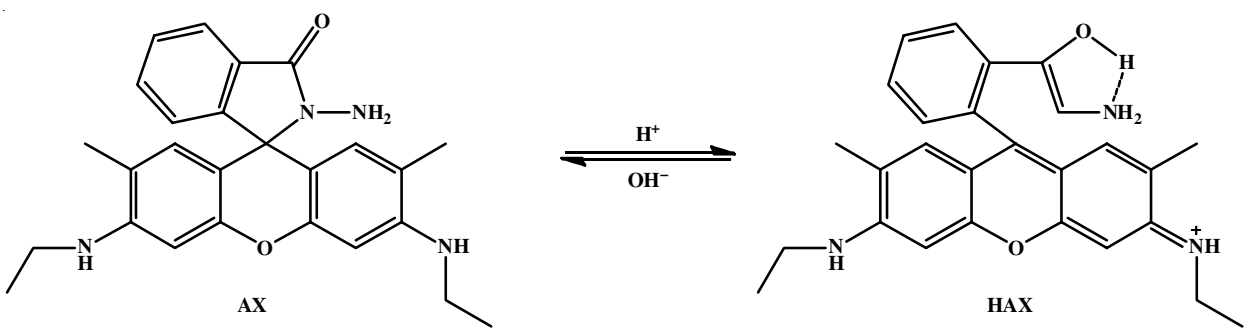

Scheme-I: Schematic diagram for acid/base induced structural conversion between AX to HAX

6-31G basis set was adopted for the present calculations. The nature of all the stationary points was confirmed by carrying out a normal mode analysis, where all vibrational frequencies were found to be positive. Time dependent density functional theory (TD-DFT) with the same B3LYP density functional was applied to study the low-lying excited states of the complex in water medium using the optimized geometries of the ground (S_0) states for the respective species. For the description of the solvent effect, both in the ground and excited states, conductor polarized continuum model (CPCM) in water medium was adapted. The vertical excitation energies of the lowest 20 singlet states were also calculated. The global minima of all these species were confirmed by the positive vibrational frequencies. The UV-Vis spectra from TD-DFT calculations were computed in the range from 250 to 700 nm in water medium.

RESULTS AND DISCUSSION

UV-Vis absorption for monitoring medium pH: UV-Vis absorption studies for AX were carried out in aqueous 40 mM Britton-Robinson buffer at various pH ranges from 1.5 to 7.0 (Fig. 1a). The visible absorption intensity centered ~ 530 nm was found to increase gradually with the decreasing pH of the buffer medium until at pH 1.5 where the intensity became saturated. The saturated absorption spectrum at the visible wavelength at highly acidic condition nicely matches with the spectrum for free unmodified rhodamine 6G. The results indicate the spirolactam ring opening and subsequent visible intensity generation due to formation of free rhodamine 6G moiety was assisted by increased acidic condition of the medium. It is interesting to observe that the generation of 530 nm visible absorption is highly advantageous to detect the pH of the medium by visible colorimetric responses (Fig. 1c). In order to estimate the pH detection more precisely, the normalized 530 nm molar extinction coefficients (each value was normalized by 530 nm intensity at pH 7.0) were plotted with the pH of the medium (Fig. 1b). The typical sigmoidal behaviour with a transition mid-point pH of ~ 4.0 can be utilized for precise estimation of unknown pH of the medium by using the following equation:

$$I_{Norm}^{530} = 1.58 - \frac{31.26}{1+\exp((pH-3.77)/0.6)}$$

It is also mentionable that more than 30-fold of intensity enhancement for the 530 nm absorption band was identified for decreasing the medium pH from 7.0 to 2.0. Moreover, the large molar extinction coefficient value for the 530 nm absorption band is highly useful for detection of minute change of pH of the medium.

Fluorescence studies for monitoring the pH of the medium: In anticipation of large fluorescence increase due to the acid induced spirolactam ring opening for the rhodamine derivative considering the UV-Vis absorption investigation, steady state fluorescence studies for AX were performed under different pH buffer medium ranging from pH 7.0 to 1.5. The non-fluorescent AX turns into highly fluorescent HAX by changing the pH of the medium from basic/neutral to acidic. The fluorescence intensity centered ~ 555 nm was found to be increased gradually by decreasing the pH of the medium. It is mentionable that about 55-fold intensity enhancement was identified for changing the medium pH from 7.0 to 1.5.

Similar founding to the absorption study, the AX fluorescence spectrum is nicely matched with the spectrum of free rhodamine 6G, which also indicates acid induced spirolactam ring opening reaction is the reason for enhancement of fluorescence intensity with decreasing pH of the medium. The large quantum yield for 555 nm fluorescence band (~ 0.5) under acidic condition is highly useful for the detection of minute variation in pH medium. To increase the analytical usefulness during the determination of unknown pH of the medium by this method, the dependencies of the fluorescence intensities on probe concentration were removed through normalizing the fluorescence intensities at various pH by the fluorescence intensity value at pH 7.0, which then plotted with pH of the medium (Fig. 2b). The analysis of fluorescence intensity changes as a function of pH by using the Henderson-Hasselbalch type mass action equation [18,19,24-26,32] yielded a pK_a of 3.9. Although the typical sigmoidal behavior was grossly followed for whole pH range from 1.5 to 7.0 but the fluorescence intensity showed a linear correlation to pH values between 2.0 and 5.5 and best fitted with the function Y = -10.076 pH + 58.217 and R^2 = 0.9889, as shown in Fig. 2c. This function further allowed us to calculate the pH value of any sample with pH ranged from 2.0 to 5.5. Therefore, probe AX could be used as a highly

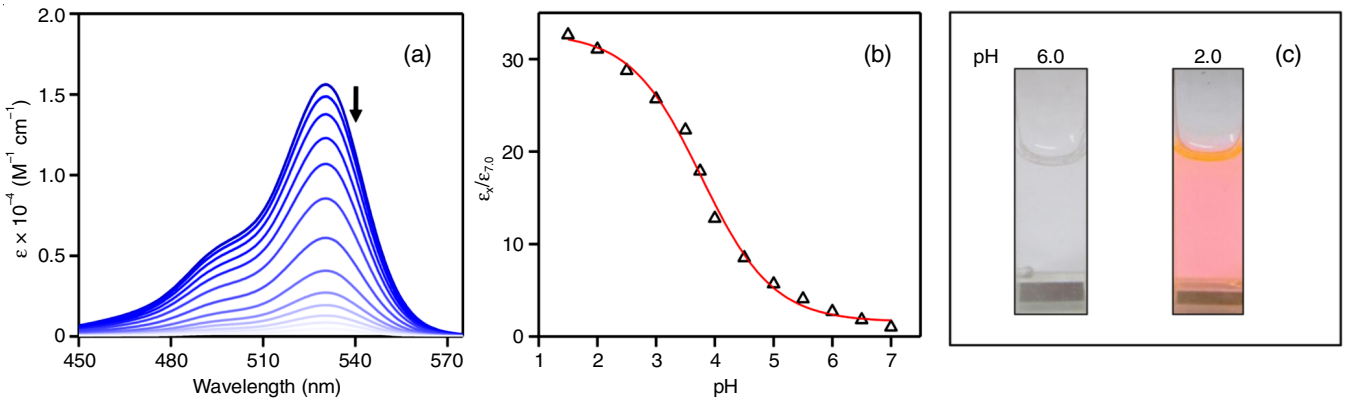

Fig. 1. (a) UV-Vis absorption spectra of AX (25.0 μM) in 40 mM buffer medium at different pH (1.5-7.0). The decrease in intensities with increase in pH is indicated by arrow; (b) Normalized molar extinction coefficient at 530 nm (ε_x) at different pH. Each ε_{530} value of different pH is normalized by dividing the molar extinction coefficient at 530 nm for pH 7.0; (c) pH dependent colorimetric responses

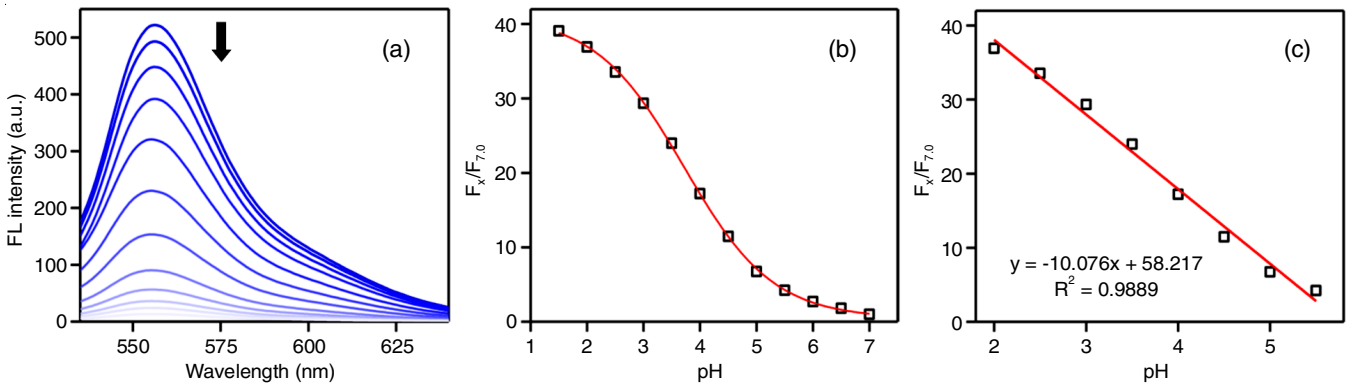

Fig. 2. (a) Steady state fluorescence spectra of AX (1.2 μM) in 40 mM aqueous buffer solution at different pH (1.5-7.0). The decrease in intensities with increase in pH is indicated by arrow; (b)The normalized fluorescence intensity ratio for different pH values (1.5-7.0) at 555 nm are plotted; (c) The normalized fluorescence at 555 nm with different pH (2.0-5.5) of the medium are plotted. The fluorescence intensity values at different pH at 555 nm are normalized by dividing the fluorescence intensity at pH 7.0. The red curve represents the linear fitting

sensitive colorimetric and fluorescent pH indicator. Since large enhancement of emission intensity due to minute variation of pH in between 2.0 to 5.5 was observed, a very small amount of pH change in this range (2.0-5.5) may be determined ratiometrically.

Fluorescence lifetime measurements: To achieve a deeper insight into the pH dependent steady state fluorescence changes, excited state fluorescence lifetime analysis for the 555 nm emission at different pH was performed. The typical decay profile is presented in Fig. 3. Single exponential behaviour for the transient decays at various pH clearly suggest that, only spirocyclic ring opening species is responsible for this fluorescence (Table-1). According to the equations: $\tau^1 = k_r + k_{nr}$ and $k_r = \Phi_f/\tau$, the radiative rate constant k_r and total non-radiative rate constant k_{nr} of the fluorophore AX at three different pH values were calculated and listed in Table-1. The insignificant change in the excited state lifetimes with single exponential character indicates that increasing the emission

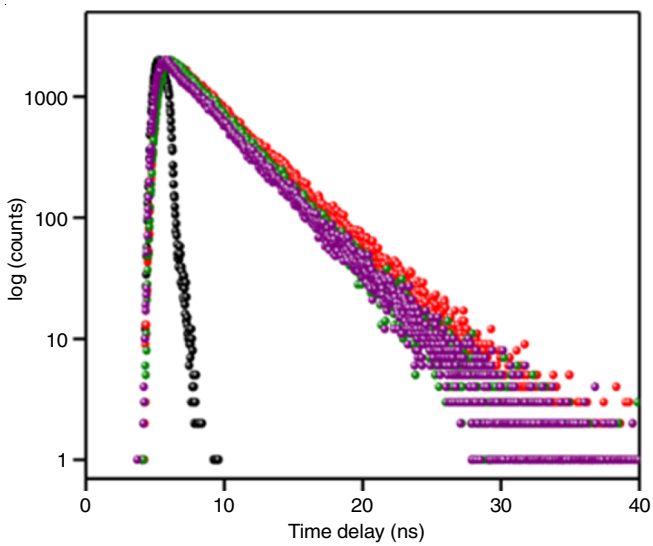

Fig. 3. Time resolved fluorescence decay curve of AX (1.2 μM) at three of different pH values in 40 mM aqueous buffer solution: red, 2.0; green, 4.0; violet, 6.0 and black, pump profile. The excitation and emission wavelength are fixed at 500 nm and 555 nm, respectively

TABLE-1
FLUORESCENCE QUANTUM YIELD (Φ_f), EXCITED STATE LIFE TIME (τ_f IN ns) AND OTHER DECAY PARAMETERS

	pH 2	pH 4	pH 6
Form	HAX	AX ↔ HAX	AX
Φ_f	0.50	0.12	0.02
τ_f (ns)	3.87	3.44	3.52
k_r (10^9 s^{-1})	0.13	0.03	0.006
k_{nr} (10^9 s^{-1})	0.12	0.26	0.28
χ^2	1.003	1.001	1.005

with decreasing the pH is not due to the presence of different excited state species but for the generation of more amount of spirolactam ring opening structure (HAX).

Reversibility of two molecular species of AX with respect to pH of the medium: To investigate the reversibility of the absorbance or the fluorescence intensity of probe AX with the pH of the medium, experiments were conducted under cyclic variation in the pH of the medium by adding HCl and NaOH solutions in a repeated fashion [19,24-26]. At first, the pH of the buffer solution for the probe HAX was changed grad-ually from 1.5 to 7.0 by adding the required amount of NaOH solution (Fig. 4). The initial absorption and emission intensities were quenched progressively when pH of the solution increased from 1.5 to 7.0. Subsequently, the pH was again reduced to pH 1.5 by gradually adding required amount of HCl solution, resulting to the complete recovery of the emission intensity. Fig. 4 also displays that when the pH is changed repeatedly between 1.5 to 7.0, both absorption and fluorescence intensity is changed by maintaining such reversibility for at least 12 occasions. These results suggest that the fluorescence or UV-Vis absorption enha-ncement/quenching of AX occur reversibly.

Theoretical studies: Ground state geometries of the AX and its protonated open form (HAX) were optimized in the gas phase by density functional theory (DFT) using Gaussian09 program [31]. The time dependent DFT (TD-DFT) studies on the optimized geometries were performed in water medium to explore the pH dependent structural analysis by correlating the experimental absorption parameters with that of theoretically obtained parameters.

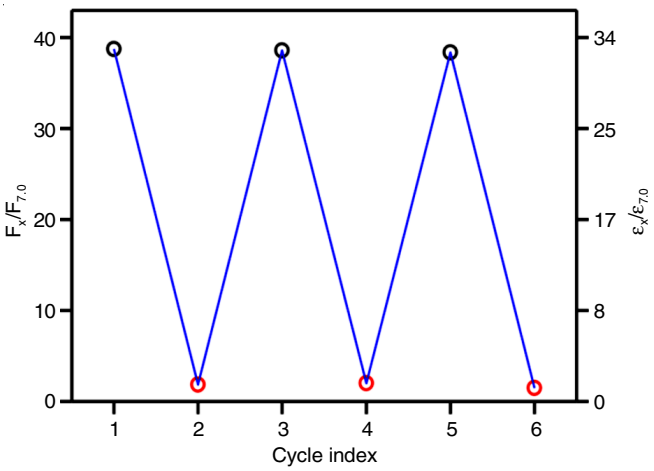

Fig. 4. pH dependent spectral reversibility plot of normalized fluorescence intensity at $\lambda_{ex/em}$ 530/555 (left y-axis) and molar extinction coefficient (right y-axis). The fluorescence intensity/ molar extinction coefficient at 555/530 nm is normalized by dividing the fluorescence intensity at pH 7.0. The pH was increased from 1.5 (black) to 7.0 (red) by an addition of 0.1 M NaOH and subsequently decreased to 1.5 (red) by an addition of 0.1 M HCl in 40 mM buffer solution

The optimized structure for protonated species (HAX) shows that the protonated amide oxygen involved intramolecular H-bonding interaction with amine nitrogen. The HOMO and LUMO electronic distribution associating with S_0 to S_1 transition for both AX and HAX are shown in Fig. 5 and the calculated HOMO and LUMO energies for the respective species are depicted in Table-2. The correlation between the experimental and the theoretically calculated absorption parameters indicate that the generation of 530 nm absorption band is due to the opening of 5-membered spirolactam ring *via* H-bonding interaction (Table-3). From the calculated HOMO and LUMO electronic distribution for the respective species, it can also be predicted that the oxygen atom of the spirolactam ring binds to H^+ ion and as a result the electron density on the xanthene ring decreases.

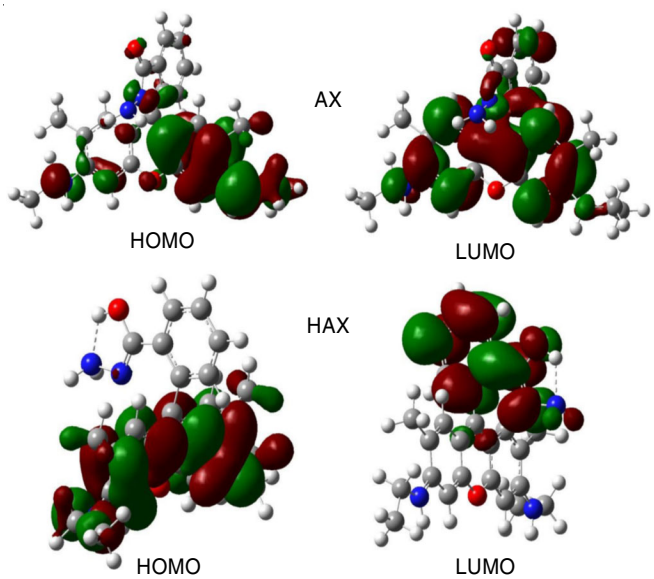

Fig. 5. Frontier molecular orbital of AX (upper panel) and HAX (lower panel) for the optimized ground states (HOMO, LUMO)

TABLE-2
HOMO AND LUMO ENERGIES

Form	E_{HOMO}	E_{LUMO}	ΔE/Ha	ΔE/eV
AX	-0.2017	-0.0430	0.159	4.327
HAX	-0.2981	0.1931	0.105	2.857

TABLE-3
COMPARISON BETWEEN EXPERIMENTAL AND CALCULATED UV-VIS ABSORPTION PARAMETERS

	Form	λ (nm)	f_{cal}	$\varepsilon \times 10^{-4}$ (M^{-1} cm^{-1})
Cal	AX	329	0.01	0.10
	HAX	490	0.15	4.39
Obs	AX	300	–	0.03
	HAX	530	–	1.56

The π-electrons on the HOMO of HAX is mainly located on the xanthene ring of rhodamine moiety, but the LUMO is positioned at the center of imide carbonyl. However, π-electrons on HOMO and LUMO of AX are mainly localized on the xanthene ring. The theoretical calculations show that deficiency of electron density occurs in the xanthene moiety due to the conversion of AX form to HAX form *i.e.* the acceptor capacity of the AX dye increases in the presence of H^+ ion. Consequently, the HOMO-LUMO energy gap for the HAX form becomes much smaller relative to that of AX form and as a result conversion of closed spirolactam ring to open spirolactam ring form easily occur.

The comparison between experimentally and theoretically calculated UV-Vis absorption parameters are summarized in Table-3. The UV spectra computed from the TD-DFT calculations in aqueous medium based on the ground state geometries are well-matched with the respective experimental spectra (Table-3).

^{1}H NMR studies: To study the protonation of AX (5 mM), the ^{1}H NMR experiments were performed in the presence of trifluoroacetic acid (TFA) (5 mM) in DMSO-d_6 (Fig. 6).

In the previous NMR studies for rhodamine 6G derivatives [33-36], it has been reported that the addition of TFA leads to a downfield shift of signals to the range 6.8-7.9 ppm from the range 6.08-7.7 ppm (for the neutral AX form in DMSO-d_6), which has been assigned due to the proton signal of xanthene moiety and thus, it indicates the delocalization effect for the xanthene moiety. Moreover, the additional new peak generated at δ =12.46 ppm (in the presence of TFA, due to the formation of intramolecular H-bonding between amide oxygen atom and amine nitrogen atom at β-position with respect to OH group) confirms the formation of HAX by protonation of AX molecule.

Conclusion

A new pH-sensitive colorimetric as well as fluorescence probe based on the derivative of rhodamine 6G was studied in the present work. It was found that when H^+ ion concentration varied in the pH range of 1.5-7.0, the probe provided a remarkable fluorescence intensity change and shows a change in its colour. The optical behaviour of probe can be tuned in off-on mode reversibly by the addition of NaOH and HCl in a cyclic fashion. The pH-dependent structural changes were discussed extensively by ^{1}H NMR studies and DFT and TD-DFT based

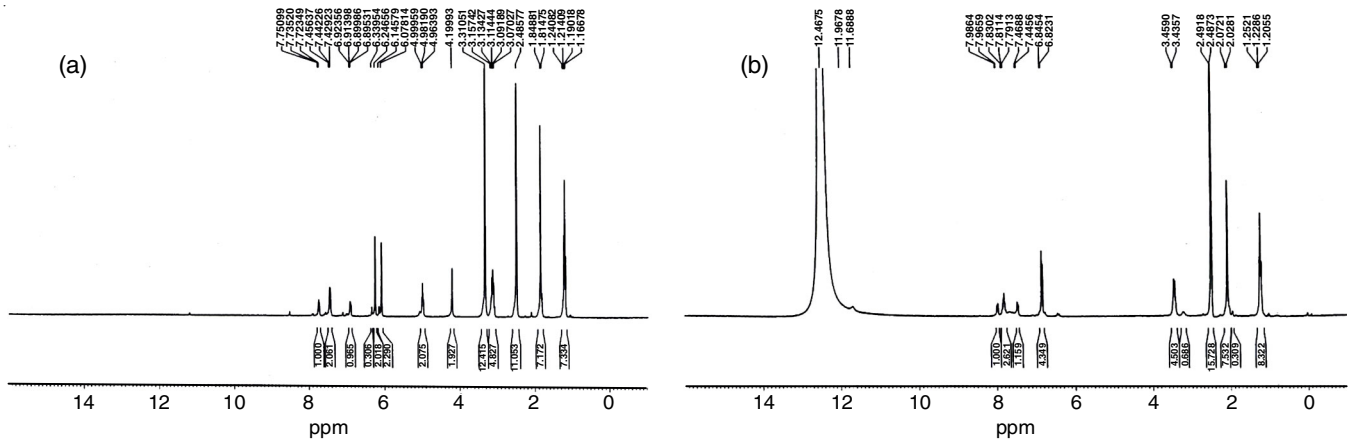

Fig. 6. ^{1}H NMR of AX (5 mM) at DMSO-d_6 solvent (a) without TFA acid (b) 5 mM TFA acid

theoretical investigations. The pH induced large change of fluorescence quantum yield can be highly beneficial for the fluorescence bioimaging studies. More specifically, the probe can be utilized with great potential for investigating the pivotal role of H^+ ion in a biological context, especially in acidic organelles through direct intracellular imaging.

CONFLICT OF INTEREST

The authors declare that there is no conflict of interests regarding the publication of this article.

REFERENCES

1. C. Das Neves Gomes, O. Jacquet, C. Villiers, P. Thuéry, M. Ephritikhine and T. Cantat, *Angew. Chem. Int. Ed.*, **51**, 1. (2012); https://doi.org/10.1002/anie.201106864
2. Y. Tan, J. Yu, J. Gao, Y. Cui, Z. Wang, Y. Yang and G. Qian, *RSC Adv.*, **3**, 4872 (2013); https://doi.org/10.1039/c3ra00120b
3. A. Kurkdjian and J. Guern, *Annu. Rev. Plant Physiol. Plant Mol. Biol.*, **40**, 271 (1989); https://doi.org/10.1146/annurev.pp.40.060189.001415
4. J. Han and K. Burgess, *Chem. Rev.*, **110**, 2709 (2010); https://doi.org/10.1021/cr900249z
5. A. Steinegger, O.S. Wolfbeis and S.M. Borisov, *Chem. Rev.*, **120**, 12357 (2020); https://doi.org/10.1021/acs.chemrev.0c00451
6. L.D. Lavis, *Biochemistry*, **60**, 3539 (2021); https://doi.org/10.1021/acs.biochem.1c00299
7. D. Wencel, T. Abel and C. McDonagh, *Anal. Chem.*, **86**, 15 (2014); https://doi.org/10.1021/ac4035168
8. L. Wu, X. Li, C. Huang and N. Jia, *Anal. Chem.*, **88**, 8332 (2016); https://doi.org/10.1021/acs.analchem.6b02398
9. X. Li, X. Gao, W. Shi and H. Ma, *Chem. Rev.*, **114**, 590 (2014); https://doi.org/10.1021/cr300508p
10. A.P. de Silva, H.Q.N. Gunaratne, T. Gunnlaugsson, A.J.M. Huxley, C.P. McCoy, J.T. Rademacher and T.E. Rice, *Chem. Rev.*, **97**, 1515 (1997); https://doi.org/10.1021/cr960386p
11. C. McDonagh, C.S. Burke and B.D. MacCraith, *Chem. Rev.*, **108**, 400 (2008); https://doi.org/10.1021/cr068102g
12. J. Krämer, R. Kang, L.M. Grimm, L. De Cola, P. Picchetti and F. Biedermann, *Chem. Rev.*, **122**, 3459 (2022); https://doi.org/10.1021/acs.chemrev.1c00746
13. X. Zhang, Y. Jiao, X. Jing, H. Wu, G. He and C. Duan, *Dalton Trans.*, **40**, 2522 (2011); https://doi.org/10.1039/c0dt01325k
14. B. Tang, X. Liu, K. Xu, H. Huang, G. Yang and L. An, *Chem. Commun.*, **3726**, 3726 (2007); https://doi.org/10.1039/b707173f
15. Z.-Q. Hu, M. Li, M.-D. Liu, W.-M. Zhuang and G.-K. Li, *Dyes Pigments*, **96**, 71 (2013); https://doi.org/10.1016/j.dyepig.2012.07.012
16. H.N. Kim, M.H. Lee, H.J. Kim, J.S. Kim and J. Yoon, *Chem. Soc. Rev.*, **37**, 1465 (2008); https://doi.org/10.1039/b802497a
17. P. Ghosh and P. Roy, *Chem. Commun.*, **59**, 5174 (2023); https://doi.org/10.1039/D3CC00651D
18. M. Tian, X. Peng, J. Fan, J. Wang and S. Sun, *Dyes Pigments*, **95**, 112 (2012); https://doi.org/10.1016/j.dyepig.2012.03.008
19. J.-L. Tan, T.-T. Yang, Y. Liu, X. Zhang, S.-J. Cheng, H. Zuo and H. He, *Luminescence*, **31**, 865 (2016); https://doi.org/10.1002/bio.3043
20. U.C. Saha, K. Dhara, B. Chattopadhyay, S.K. Mandal, S. Mondal, S. Sen, M. Mukherjee, S. van Smaalen and P. Chattopadhyay, *Org. Lett.*, **13**, 4510 (2011); https://doi.org/10.1021/ol201652r
21. R. Gui, X. An and W. Huang, *Anal. Chim. Acta*, **767**, 134 (2013); https://doi.org/10.1016/j.aca.2013.01.006
22. B.K. McMahon, R. Pal and D.A. Parker, *Chem. Commun.*, **49**, 5363 (2013); https://doi.org/10.1039/c3cc42308e
23. H.S. Lv, S.Y. Huang, B.X. Zhao and J.Y. Miao, *Anal. Chim. Acta*, **788**, 177 (2013); https://doi.org/10.1016/j.aca.2013.06.038
24. X.X. Zhao, X.P. Chen, S.L. Shen, D.P. Li, S. Zhou, Z.Q. Zhou, Y.H. Xiao, G. Xi, J.-Y. Miao and B.X. Zhao, *RSC Adv.*, **4**, 50318 (2014); https://doi.org/10.1039/C4RA07555B
25 X.-F. Zhang, T. Zhang, S.-L. Shen, J.-Y. Miao and B.-X. Zhao, *J. Mater. Chem. B Mater. Biol. Med.*, **3**, 3260 (2015); https://doi.org/10.1039/C4TB02082K
26. S.-L. Shen, X.-F. Zhang, S.-Y. Bai, J.-Y. Miao and B.X. Zhao, *RSC Adv.*, **5**, 13341 (2015); https://doi.org/10.1039/C4RA16398B
27. W. Luo, H. Jiang, X. Tang and W. Liu, *J. Mater. Chem. B Mater. Biol. Med.*, **5**, 4768 (2017); https://doi.org/10.1039/C7TB00838D
28. W. Zhang, B. Tang, X. Liu, Y. Liu, K. Xu, J. Ma, L. Tong and G. Yang, *Analyst*, **134**, 367 (2009); https://doi.org/10.1039/B807581F
29. S. Kang, S. Kim, Y.-K. Yang, S. Bae and J. Tae, *Tetrahedron Lett.*, **50**, 2010 (2009); https://doi.org/10.1016/j.tetlet.2009.02.087
30. C. Wurth, M. Grabolle, J. Pauli, M. Spieles and U. Resch-Genger, *Anal. Chem.*, **83**, 3431 (2011); https://doi.org/10.1021/ac2000303
31. M.J. Frisch, G.W. Trucks, H.B. Schlegel, G.E. Scuseria, M.A. Robb, J.R. Cheeseman, G. Scalmani, V. Barone, G.A. Petersson, H. Nakatsuji, X. Li, M. Caricato, A. Marenich, J. Bloino, B.G. Janesko, R. Gomperts,

B. Mennucci, H.P. Hratchian, J.V. Ortiz, A.F. Izmaylov, J.L. Sonnenberg, D. Williams-Young, F. Ding, F. Lipparini, F. Egidi, J. Goings, B. Peng, A. Petrone, T. Henderson, D. Ranasinghe, V.G. Zakrzewski, J. Gao, N. Rega, G. Zheng, W. Liang, M. Hada, M. Ehara, K. Toyota, R. Fukuda, J. Hasegawa, M. Ishida, T. Nakajima, Y. Honda, O. Kitao, H. Nakai, T. Vreven, K. Throssell, J.A. Montgomery, Jr., J.E. Peralta, F. Ogliaro, M. Bearpark, J.J. Heyd, E. Brothers, K.N. Kudin, V.N. Staroverov, T. Keith, R. Kobayashi, J. Normand, K. Raghavachari, A. Rendell, J.C. Burant, S.S. Iyengar, J. Tomasi, M. Cossi, J.M. Millam, M. Klene, C. Adamo, R. Cammi, J.W. Ochterski, R.L. Martin, K. Morokuma, O. Farkas, J.B. Foresman and D.J. Fox, Gaussian 09, Revision A.02, Gaussian, Inc., Wallingford CT (2016).

32. Q.A. Best, R. Xu, M.E. McCarroll, L. Wang and D.J. Dyer, *Org. Lett.*, **12**, 3219 (2010); https://doi.org/10.1021/ol1011967
33. Y. Mi, Z. Cao, Y. Chen, S. Long, Q. Xie, D. Liang, W. Zhu and J. Xiang, *Sens. Actuators B Chem.*, **192**, 164 (2014); https://doi.org/10.1016/j.snb.2013.10.103
34. M. Dong, T.H. Ma, A.J. Zhang, Y.M. Dong, Y.W. Wang and Y. Peng, *Dyes Pigments*, **87**, 164 (2010); https://doi.org/10.1016/j.dyepig.2010.03.015
35. P. Mahato, S. Saha, E. Suresh, R. Di Liddo, P.P. Parnigotto, M.T. Conconi, M.K. Kesharwani, B. Ganguly and A. Das, *Inorg. Chem.*, **51**, 1769 (2012); https://doi.org/10.1021/ic202073q
36. H. Zheng, Z.H. Qian, L. Xu, F.F. Yuan, L.D. Lan and J.G. Xu, *Org. Lett.*, **8**, 859 (2006); https://doi.org/10.1021/ol0529086